



The Co-evolution of QSOs and Galaxies

Roger Coziol, Juan Pablo Torres-Papaqui, Heinz Andernach

Depto. de Astronomía, Univ. Guanajuato, Mexico

rcoziol, papaqui, heinz@astro.ugto.mx

Back at the Edge of the Universe :
Latest results from the deepest
astronomical surveys,
Sintra, Portugal, March 15–19, 2015

ABSTRACT Using two large samples of QSOs detected in the mid-infrared (MIR) with WISE, we find that the change of W2–W3 colors with redshift suggests that star formation in their host galaxies increases by a factor of 3 from $z = 0$ to $z = 2.7$, then stays constant up to $z = 4$, and decreases above $z=4$. This behavior is slightly different from the best fits for the star formation history of field galaxies as deduced from the Optical-UV and IR, but is consistent with what is observed for sub-mm galaxies at high z . Our results constitute the clearest evidence, so far, that QSO host galaxies form their stars before field galaxies, and are in good agreement with the hierarchical biased structure formation paradigm.

1. Introduction

In 1998, Madau, Pozzetti & Dickinson [1] published one comprehensive view about the cosmic star formation history (SFH) of field galaxies, as determined from deep spectroscopic samples and the Hubble Deep Field imaging survey. Their curve for the evolution of the density of star formation at different redshifts shows a strong increase of star formation, by a factor of 10, from $z = 0$ to $z \approx 2$, followed by a slower decrease for $z > 2$.

The same year, Boyle and Terlevich [2] showed that the luminosity density of QSOs at different redshifts follows a comparable evolutionary curve, and suggested that a substantial fraction of the emitted luminosity in the optical-UV spectrum of QSOs must be associated with star formation. If this is true, then a substantial fraction of the emission in IR in QSOs must also be due to star formation.

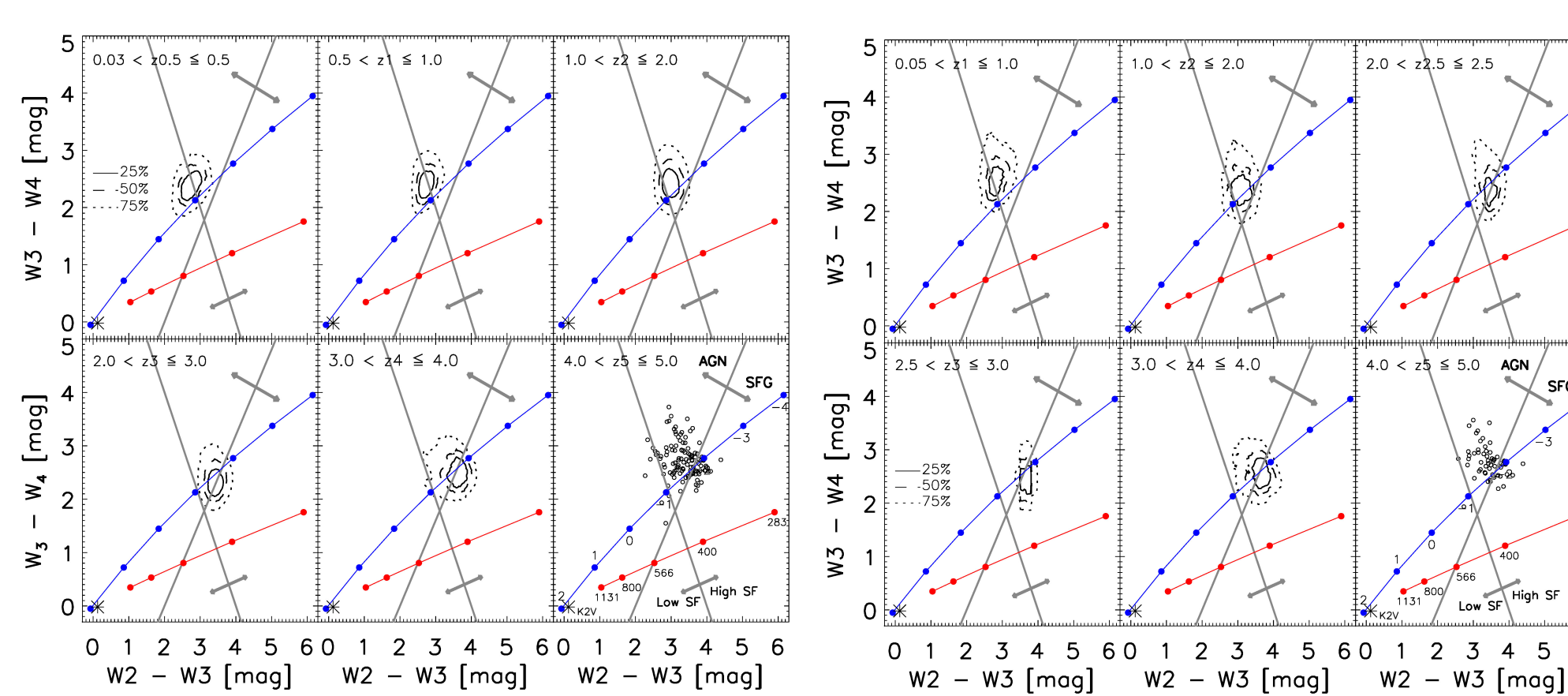
Consistent with the above interpretation, we [3] recently demonstrated that the WISE mid-infrared (MIR) W2–W3 color is, indeed, a good tracer of star formation at low redshift ($z \leq 0.25$) in emission-line galaxies with different activity types: star forming galaxies (SFGs), Transition type Objects (TOs), Low-Ionisation Narrow Emission-line Regions (LINERs), Seyfert 2 (Sy2s) and Seyfert 1 (Sy1s), BL Lac objects and QSOs. By comparing the colors of these galaxies, it was inferred that in the nearby universe star formation increases along the sequence BL Lac \rightarrow LINER \rightarrow QSO/Sy1 \rightarrow Sy2 \rightarrow TO \rightarrow SFG.

Following the same line of thought, if the W2–W3 color of QSOs is related to star formation, then one would expect their colors to change at high redshift in a way that would imply an increase of star formation, and which would be consistent with the SFH. This is what we verify in this poster.

2. Samples of QSOs

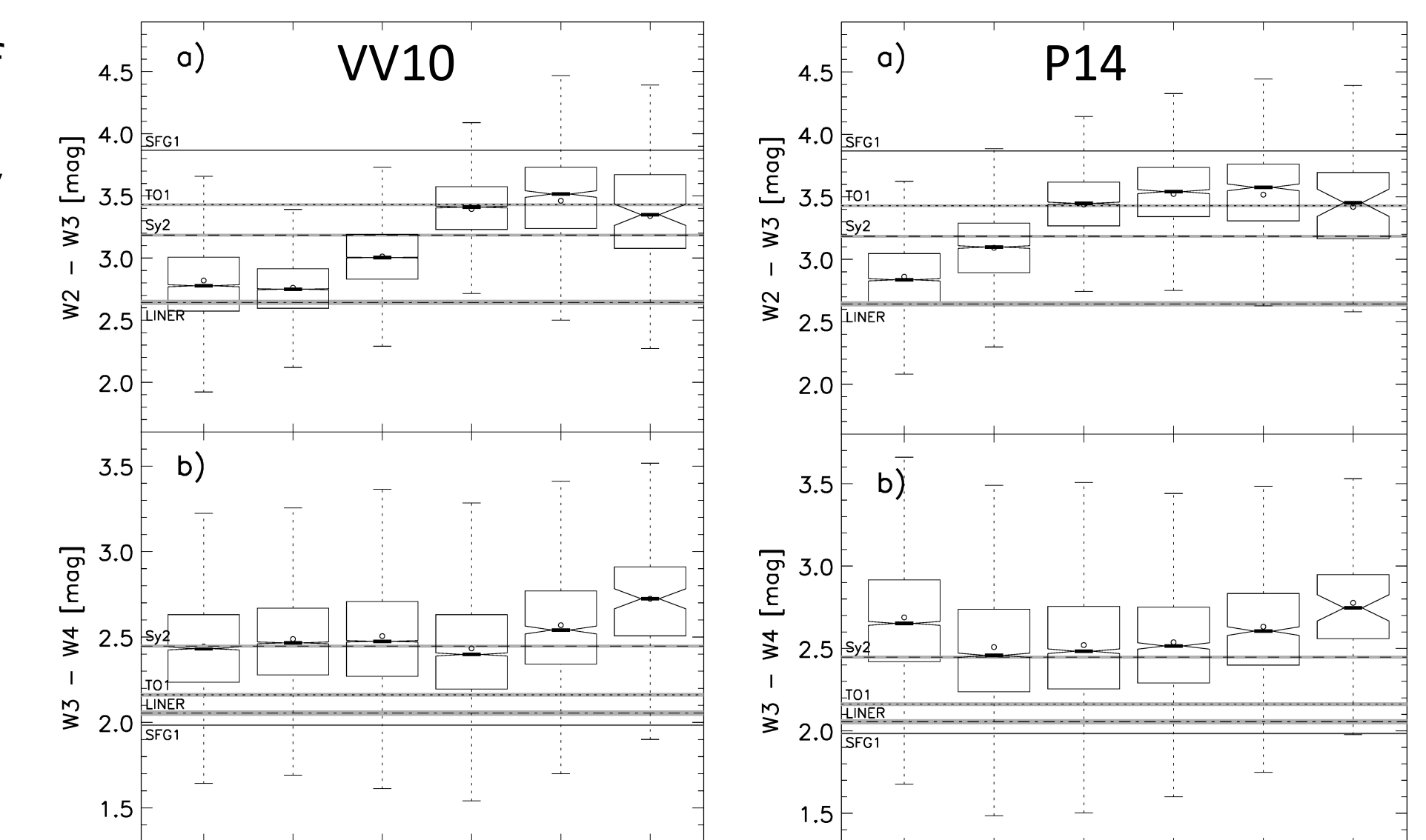
To test our hypothesis, we selected two large samples of QSOs: the catalog of quasars and active nuclei by Véron-Cetty & Véron (13th ed.; VV10 [4]), and the Sloan Digital Sky Survey DR10 QSO catalog (Pâris et al. 2014, P14 [5]). We cross-correlated the positions of the QSOs in each catalog with the positions of the entries in the WISE All-Sky Release Source Catalog [6], using the X-Match pipeline in Vizier [7]. Keeping only the QSOs that have WISE fluxes with S/N > 3 in the four WISE filters, 3.4 μ m (W1), 4.6 μ m (W2), 12 μ m (W3) and 22 μ m (W4), we obtained 25,505 QSOs from VV10 and 14,517 QSOs from P14.

3. MIRDD of QSOs at different redshifts

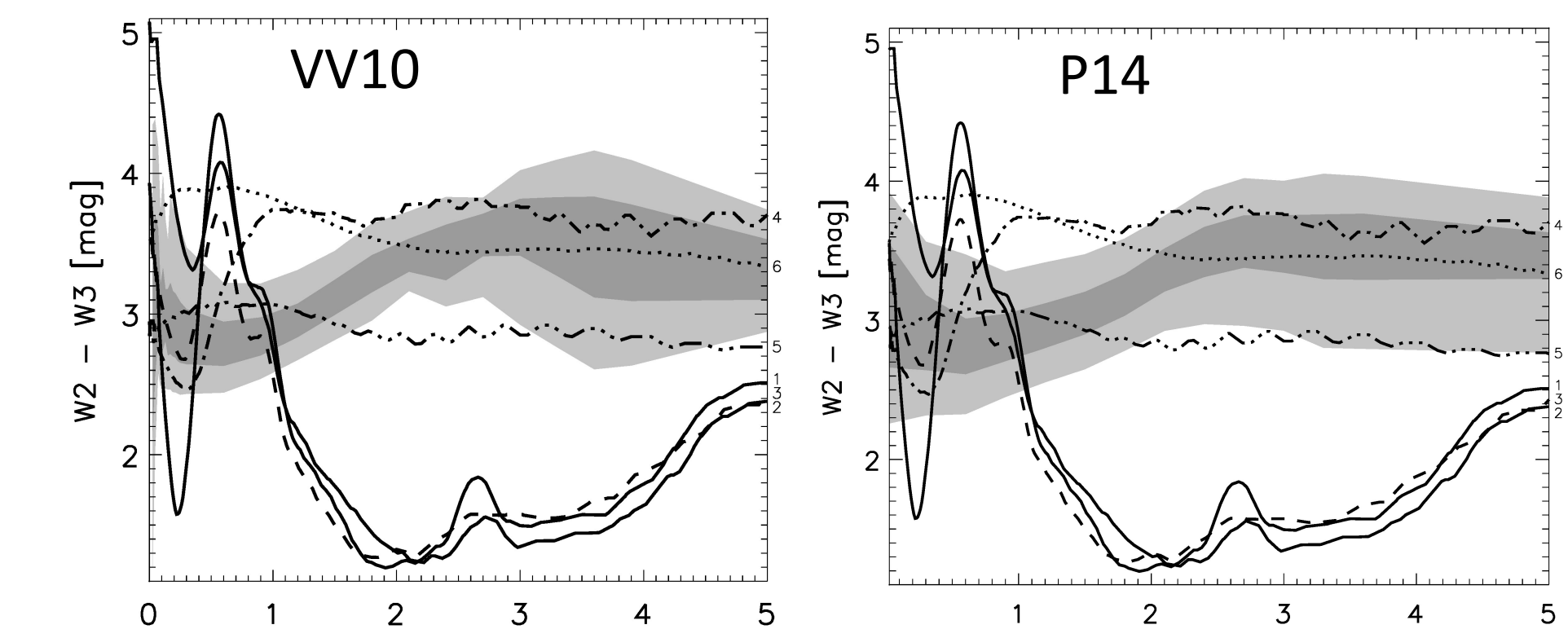


In the above figures, we compare the colors of the QSOs in the MIR diagnostic diagram, MIRDD [3]. In all the figures, VV10 is on the left panel and P14 is on the right. The QSOs are separated in six different redshift bins. The VV10 has more QSOs between $z = 0$ and 1 than the P14 QSOs, but is less complete at intermediate redshift. In both samples, the positions of the QSOs in the MIRDD gradually move towards the region occupied by the SFGs, which is consistent with an increase of star formation at higher redshift.

The box-whisker plots below clearly show the changes of W2–W3 colors of QSOs at higher redshift, while the W3–W4 colors stay almost constant. In the VV10 sample, star formation reaches its maximum between $z = 3$ and $z = 4$, while the SFR in the P14 sample forms a plateau, extending from $z = 2$ to $z \approx 4$. In both samples, the SFR decreases for $z > 4$.

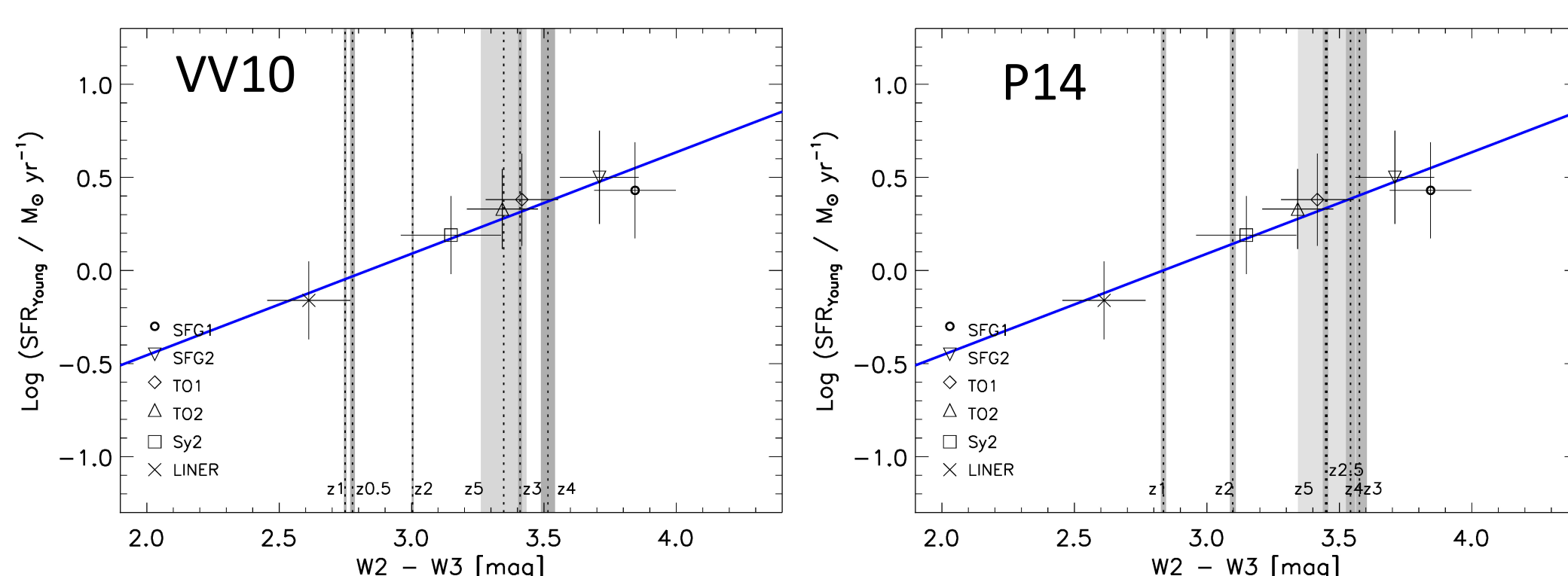


4. Comparison with SEDs



In the above figures, the variation of the W2–W3 colors of QSOs (grey areas) is compared with the variations predicted by different SEDs, drawn as lines [3]: #1 and #2 are the SEDs of two starburst galaxies, #3 is a Sy2, #4 is a Sy1, #5 is a QSO with low star formation rate (SFR) and #6 is a QSO with a high SFR [8]. The best fitted SED is #5 at low z , changing to #6 at high z , implying that star formation in QSOs increases with increasing z .

5. Calibration of W2–W3 in terms of SFR



In the above figures, we show the variations of the W2–W3 color of QSOs in different redshift bins, as observed in the VV10 (left) and P14 (right) sample, comparing them with the median colors of narrow emission-line galaxies (NELGs) with different activity types. For the latter we determined their SFR by performing a stellar population synthesis on their SDSS spectra [3]. The W2–W3 colors of the NELGs suggests an increase of star formation by a factor 10 along the sequence LINER \rightarrow Sy2 \rightarrow TO \rightarrow SFG.

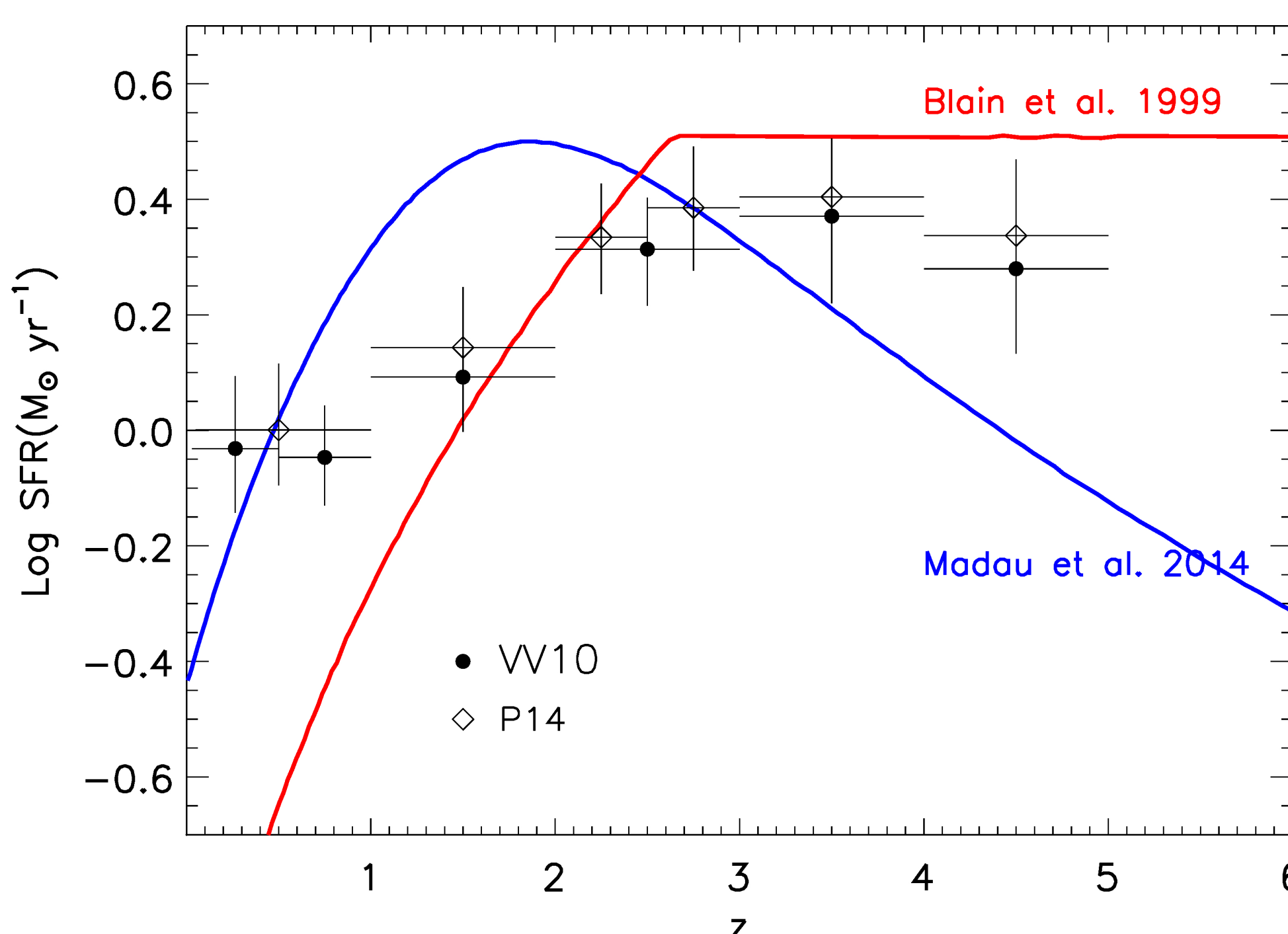
The above comparison led us to a best-fitting relation between W2–W3 and SFR as follows: $\log \text{SFR}(M_{\odot} \text{ yr}^{-1}) = 0.545 (W2-W3) - 1.545$. Applying this relation to the colors of QSOs, we deduce the SFRs at different redshifts. The values are compiled in Table 1 below.

VV10 sample		P14 sample	
z	$\text{Log SFR}(M_{\odot} \text{ yr}^{-1})$	z	$\text{Log SFR}(M_{\odot} \text{ yr}^{-1})$
$.03 \leq z < 0.5$	-0.03 ± 0.12	$0.05 \leq z < 1.0$	0.00 ± 0.12
$.05 \leq z < 1.0$	-0.05 ± 0.09	$1.0 \leq z < 2.0$	0.14 ± 0.25
$1.0 \leq z < 2.0$	0.09 ± 0.10	$2.0 \leq z < 2.5$	0.33 ± 0.43
$2.0 \leq z < 3.0$	0.31 ± 0.09	$2.5 \leq z < 3.0$	0.38 ± 0.49
$3.0 \leq z < 4.0$	0.37 ± 0.13	$3.0 \leq z < 4.0$	0.40 ± 0.50
$4.0 \leq z < 5.0$	0.28 ± 0.16	$4.0 \leq z < 5.0$	0.34 ± 0.47

Our calibration suggests that the SFR of QSOs increases by a factor ≈ 3 from $z = 0.3$ to $z = 3.5$. There is also a clear trend in both samples suggesting that the SFR in QSOs decreases above $z = 4$.

6. Tracing the SFH of QSOs

In the figure below, we trace the SFH of the QSOs as deduced from their W2–W3 colors at different redshifts. We also show the SFH of field galaxies (in blue) as determined by Madau and Dickinson [9], scaling up their relation to fit the maximum SFR in SFGs. At low redshift the SFH of the QSOs is in good agreement with the SFH of field galaxies. However, their SFR at higher redshift is below the SFH of the field galaxies, and the QSOs reach their maximum SFR at higher redshift ($z \approx 2.7$, instead of 1.9). Moreover, the SFR of QSOs stays constant up to a redshift of 4, instead of decreasing just after its maximum.



In 1999, Blain et al. [10] produced a different SFH based on SCUBA sub-mm observations, suggesting that a high fraction of star forming galaxies at high redshift were not taken into account by the optical-UV SFH. They proposed a different SFH which we show as a red curve in our figure (scaled to the SFR of SFGs). The important new feature of this SFH is a constant SFR after the maximum at $z \approx 2.7$, which is close to what we see for the SFH of the QSOs.

Our results suggest that QSOs formed their stars before the field galaxies. It seems natural, therefore, to see their SFRs falling before the maximum of SFR in field galaxies. Our results also suggest that star formation in QSOs contributes in explaining the sub-mm observations, at high redshift, in good agreement with recent results obtained by Serjeant et al. [11].

7. Conclusions

- The W2–W3 colors of QSOs systematically become redder at higher redshift, which is consistent with an increase of star formation in their host galaxies [3].
- A comparison of the change of W2–W3 colors in QSOs with the change of colors predicted by different SEDs supports this: a higher level of star formation is needed to explain the SEDs of QSOs at high redshift [8].
- This confirms that a substantial fraction of the emission in MIR in QSOs must be due to star formation in their host galaxies [2,3].
- By calibrating the W2–W3 colors in terms of SFR, we have deduced the SFH of QSOs, finding that it differs from the SFH of field galaxies. The maximum SFR in QSOs occurs at a higher redshift, implying that QSOs must have formed their stars before these galaxies.
- The SFH of QSOs at high redshift is similar to the SFH of galaxies inferred from sub-mm data [10], suggesting that star formation in QSOs plays an important role in explaining these observations [11].

Within the hierarchical biased structure formation paradigm, massive galaxies form first in massive structures, while less massive galaxies in the field form later. Assuming that the process of galaxy formation is tightly connected to the formation of a black hole (BH) at their center, one would expect more massive BHs to form before less massive ones, which would explain the difference between the SFH of field galaxies and that of QSOs.

8. References

- [1] Madau, P., Pozzetti, L., & Dickinson, M. 1998, ApJ, 498, 106
- [2] Boyle, B.-J., & Terlevich, R.-J. 1998, MNRAS, 293, L49
- [3] Coziol, C., Torres-Papaqui, J. P. & Andernach, H. 2015, AJ, (Submitted)
- [4] Véron-Cetty, M.-P. & Véron, P. 2010, A&A, 518, 10
- [5] Pâris I., et al. 2014, A&A, 563, A54
- [6] Cutri, R. M. et al. 2013, Vizier Online Data Catalog: AllWISE Data Release (2013yCat.2328...0C)
- [7] Ochsenbein, F., Bauer, P. & Marcout, J. 2000, A&AS, 143, 23
- [8] Leipski, C. et al., 2014, ApJ, 785, 154
- [9] Madau, P. & Dickinson, M. 2014, ARA&A, 52, 415
- [10] Blain, A.W. et al. 1999, MNRAS, 302, 632
- [11] Serjeant, S. et al. 2010, A&A, 518, L7